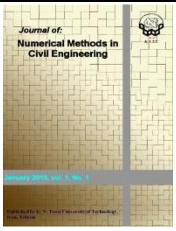

Numerical Methods in Civil Engineering

An enhanced BEM approach applied to potential problems: a comparative study

Parham Azhir[*], Jafar Asgari Marnani[**], Mehdi Panji [***], and Mohammad Sadegh Rohanimanesh[****]

ARTICLE INFO
Article history:
Received:
May 2020.
Revised:
July 2020.
Accepted:
September 2020.
Keywords:
Boundary Element Method (BEM); Singularity; Logarithmically Singular Functions; Numerical Integration; Gauss Quadrature; Fundamental Solution

Abstract:

In the present paper, a hybrid analytical/numerical method capable of integrating singular logarithmic functions, as an essential part of the Boundary Element Method (BEM) process, is presented. The proposed scheme provides a more practical approach through the reduction of the computational effort of the analytical method. For this purpose, the singular function is divided into two parts of singular and non-singular. The non-singular part is numerically integrated, while the singular part is analytically integrated and the result of both parts is combined. The capabilities and accuracy of the proposed scheme are investigated through various elemental and potential examples. The results of numerical comparisons indicate the ability of the proposed scheme to reduce the computational effort of the analytical solutions, which develops an appropriate alternative for the simple analytical solution of the potential problems that can be used in practical modeling problems such as heat transfer.

1. Introduction

Various numerical methods have been developed based on the weighted residuals [1-4]. Regardless of the advantages and disadvantages of each one, the most conventional methods are the Finite Elements Method (FEM) [5, 6] and the BEM [7-11], respectively. Recently, due to specific features of the BEM, especially in the modeling of semi-infinite and infinite fields and the possibility of cooperation with the FEM, further attention has been raised in this field [12, 13]. Continuous investigations of researchers indicate potential possibilities of the BEM method in the investigation of far filed problems such as shallow tunnels [14, 15] and crack propagation analysis [16-19], where the brittle materials crack branching mechanism has been analyzed.

* *Department of Civil Engineering, Central Tehran Branch, Islamic Azad University, Tehran, Iran.*
** *Corresponding Author: Department of Civil Engineering, Central Tehran Branch, Islamic Azad University, Tehran, Iran. E-mail: j_asgari@iauctb.ac.ir*
*** *Department of Civil Engineering, Zanjan Branch, Islamic Azad University, Zanjan, Iran.*
**** *Department of Civil Engineering, Central Tehran Branch, Islamic Azad University, Tehran, Iran.*

The proelastic fundamental solutions of the displacement discontinuity method are also presented by focusing on the behavior of cracks induced due to various methods such as boring by explosion or boring machinery. On the other hand, the BEM can be extended to the half-plane time-domain boundary element method in which only the boundary of the interface of the structures needs to be discretized and through satisfactions of the continuity and boundary conditions, it can be used as a hybrid of the normal BEM and half plane BEM. Further details can be found in [20-22] where practical capacities of BEM and hybrid BEM for analyzing of site response is investigated.

Besides significant advantages of the BEM such as accuracy of the method in the modeling of far field domains such as soil domain and reduction of degrees of the space by one, a big disadvantage of the BEM is the treatment of the singular integrals, which appear in the process of formulation. Various studies carried out until now have addressed the problem of integrating logarithmically singular functions of the BEM and led to several methods of integration on singular functions [23, 24]. Each one of these methods has its pros and cons.

Analytical methods of integration can solve singular integrals. However, the problem is that these methods are not capable of integrating all functions efficiently and preparation of the large number of codes by means of these methods is time consuming and cannot be used to overcome engineering problems. In general, numerical integrals are more common and thus capable of solving engineering problems, however, specific attention and comparison of results and capabilities are required.

Many researchers have proposed different numerical methods specifically developed for numerical integration of singular integrals. Crow [23] has proposed a numerical method for the integration of logarithmically singular integrals. Some of the researchers have compared the existing methods, for example, Smith [24] has compared some of the proposed integration methods for logarithmically singular integrals. Also, some other researchers have proposed hybrid methods, for example, Sladek, et al. [25] proposed a semi analytical integration method for the integration of nearly logarithmically singular integrals.

Analytical models often do not perform well for the real complex field scale situation. Various numerical simulation models, including continuum-based models such as finite element methods and dis-continuum models such as distinct element methods, have been proposed by various researchers [18]. Marji, et al. [26] investigated the crack propagation mechanism in rocks using the Higher Order Displacement Discontinuity Method (HODDM) with special crack tip elements. Also, a complete analytical, experimental, and numerical analysis of crack propagation, and cracks coalescence in rocks and rock-like materials under compressive loading condition have been performed by Haeri, et al. [27].

Several studies have investigated and described numerical and analytical integration methods and compared their advantages and disadvantages with well-known schemes such as GAUSS and SIMPSONS [28], while some others have addressed instability of the results due to integration methods and have proposed various numerical stepping schemes [29]. However, the investigation of singular integration has gained minimal attention. Representation of the singular terms, which in practice is performed through various quadrature methods in different papers, has been investigated by analytical methods such as [30] Some researchers have addressed the exact solution of the BEM matrixes. Their activities concentrated on 2 and 3 dimensional elements for the singular and nonsingular integrations [31].

The function to be integrated can influence the behavior of the integrating approaches. In all the above-mentioned papers, researchers have used simple functions for illustration of their integrating methods capabilities. While in this paper, a common fundamental function of the BEM is used to compare the capabilities of the integration schemes. The main contributions of this paper are stated as follows:

1. Comparison of the existing methods on the integration of fundamental functions.
2. Improving BEM solutions by proposing a proper integration method for singular and semi singular conditions.
3. Comparison of the accuracy of various integration methods.

2. Laplace equation

One of the most important partial differential equations in mathematical physics is the Laplace equation, which has wide applications in engineering fields, such as fluid flow and heat conduction, where all those fields can be represented by a potential gradient. The Laplace equation can be derived from several physical processes. Further details can be found in [32] where the Laplace equation is derived for the fluid flow field as equation 1:

$$\nabla^2 u = 0$$
$$\nabla^2 = \frac{\partial^2}{\partial x^2} + \frac{\partial^2}{\partial y^2} + \frac{\partial^2}{\partial z^2} \quad (1)$$

Where ∇^2 is the Laplace equation as $\mathrm{div}[\nabla]$ and u is the potential function of the field. The natural and essential boundary conditions of the problem can be identified as follows:

$$essential\ conditions\ as\ u = \bar{u}\ on\ \Gamma_1$$
$$natural\ conditions\ as\ q = \frac{\partial u}{\partial n} = \bar{q}\ on\ \Gamma_1$$

Where n is normal to the boundary and the total boundary Γ is constituted of the essential and the natural boundaries of $\Gamma = \Gamma_1 + \Gamma_2$ as indicated in Fig. 1.

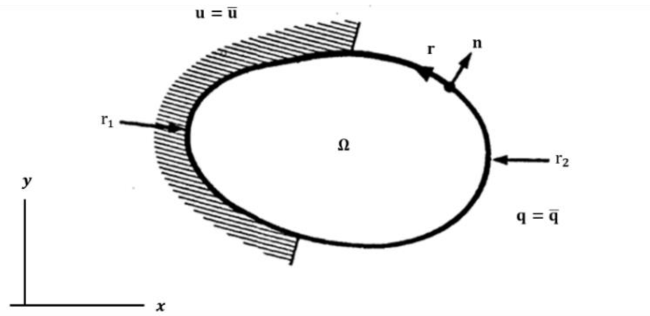

Fig. 1: The natural and the boundary conditions for an arbitrary Laplace problem

2. 1. Integral equation

Considering the Laplace equation (equation 1) and the weighted residual method besides integration by parts [9], basic integral equations for the BEM is derived as equation2:

$$\int_{\Omega} (\nabla^2 u^*) u \, d\Omega = -\int_{\Gamma_2} \bar{q} u^* \, d\Gamma - \int_{\Gamma_1} q u^* d\Gamma + \int_{\Gamma_2} u q^* d\Gamma + \int_{\Gamma_1} \bar{u} q^* d\Gamma \quad (2)$$

Where Ω is the control field and uppercase * indicates the weighted functions.

2. 2. Fundamental solution

The fundamental solution for an arbitrary operator L is defined as the solution of equation 3 considering Dirac delta on the right hand side of the equation.

$$L(u) = -\delta \tag{3}$$

Where δ is the Dirac delta function and the Laplace equation yields equation 4.

$$\nabla^2 u^* + \delta = 0 \tag{4}$$

The solution of equation 4 for a 3 dimensional case leads to the fundamental solution of the Laplace equation as indicated in equation 5 and further details can be found in [9].

$$u^* = \frac{1}{4\pi r} \tag{5}$$

Where r is the distance between the source point and the colocation point, and for a 2 dimensional case, the solution is as equation 6.

$$u^* = -\frac{1}{2\pi} \cdot \ln(r) \tag{6}$$

As indicated in equation 6 tending r to zero, and placing source point on the colocation point, the fundamental solution tends to infinity, which leads to the singular case of the integrations in the BEM method.

3. Analytical solution

One of the capabilities of MATLAB programming language is to integrate predefined function analytically. Due to time consuming specification of this feature, its usage for the integration of fundamental singular functions of the BEM formulation is not feasible. The function can be treated as a general analytical solution for comparison of the results with the exact results of an analytical integration of the fundamental solution. In this paper analytical solutions developed by MATLAB have been used to integrate the functions analytically, and the results of other methods have been compared with the result of the proposed integration scheme.

3. 1. Fundamental solution and singularities

A fundamental solution is the solution of the potential problem for a unit applied concentration of potential at a source point. An upper star mostly indicates the fundamental solution and its derivatives. Here, the Laplace equation is addressed, thus its fundamental and derivatives of the fundamental solution for a 2D case are further used as the part of integral which produces logarithmic singularity. The fundamental solution and its normal derivative are presented as follows [9, 33]:

$$u^* = -\frac{1}{2\pi} \cdot \ln(r) \tag{7}$$

$$q^* = -\frac{1}{2\pi r}\,(r_{,1}.n1 + r_{,2}.n2) \tag{8}$$

Where r is the distance between the source point and an arbitrary point on the boundary, $r_{,1}$, and $r_{,2}$ are derivatives of the r with respect to x and y coordinates and n1, and n2 are normal of the boundary in the x and y coordinates. If r tends to zero, $ln(r)$ tends (also) to infinity which creates a singularity in the integral. To integrate such integrals, some specific techniques shall be used. In the following, two of these techniques are compared and a numerical code is developed for each one.

Due to the behavior of $ln(r)$ in the function of $u^*\phi_i$, which is a very common function in the BEM, when r→ 0, the $u^*\phi_i$ tends to the logarithmic singular function. Where u^* is the fundamental solution and ϕ_i is the shape function (which will be later discussed). Integration of this function requires specific attention and normal approaches are insufficient in this case. Therefore a specific integration method is compared with the analytical result obtained by the MATLAB programming language.

$$u^*\phi_i \tag{9}$$

3. 2. Natural coordinate

The first step is to introduce the natural coordinate system such that, the value of "t" at the first node of the element is -1 and at the last node is +1. Generally, this coordinate can address curved elements, but here the elements are assumed to be linear. Fig. 2 illustrates a typical three-node curved element with a local natural coordinate system which is laid along with the element.

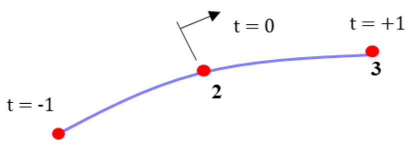

Fig. 2: Local coordinate system laid on a typical element

3. 3. Iso-parametric shape functions

Quadratic shape functions are used to define the variation of the boundary values and Cartesian coordinates of each element's point. Using the previously mentioned local coordinate system of $t[-1,+1]$, shape functions will be formulated as follows [9]:

$$\phi_1 = -0.5\,t\,(1 - t) \tag{10}$$

$$\phi_2 = (1 + t)\cdot(1 - t) \tag{11}$$

$$\phi_3 = 0.5\,t\,(1 + t) \tag{12}$$

Where ϕ_i, the shape function with respect to the node number i and t indicates the natural coordinate value. Also, the 2D Cartesian coordinate system values, x and y, for each element's point can be defined as follows:

$$x = \phi_1 x_1 + \phi_2 x_2 + \phi_3 x_3 \tag{13}$$

$$y = \phi_1 y_1 + \phi_2 y_2 + \phi_3 y_3 \quad (14)$$

Where x_i and y_i, $i = 1, 2$ and 3, are nodal values of x and y respectively. Using these coordinates, the distance between the boundary point and an arbitrary point (xs, ys) can be defined as follows:

$$r = \sqrt{(x - xs)^2 + (y - ys)^2} \quad (15)$$

3. 4. Derivatives with respect to natural coordinates

As integration is performed in a local (natural) coordinate system, transformation of a variable shall be performed. Jacobean of transforming to the natural coordinates is presented as follows:

$$J = \sqrt{dxt^2 + dyt^2} \quad (16)$$

Where dxt and dyt are derivatives of x and y with respect to the natural coordinate system value, respectively. Using the above mentioned equations, the formulation for integrating function of $u^*\phi_1$ represented by G is as follows:

$$G = \int_{-1}^{+1} u^* \phi_1 J dt \quad (17)$$

An analytical formulation can integrate the logarithmic singular function of $u^*\phi_\text{i}$ accurately, dues a code has been developed through the analytical functions in MATLAB. It is notable that in this specific case singularity is adopted at point 1 where the source point lies on the boundary node.

4. Derivation of G by normal Gauss quad (10 point)

For evaluating and comparing the precision of the introduced approach, in the first step, normal Gauss quad integration is used. Formulation of normal gauss quad for arbitrary boundary values from point of “a” to “b” is as follows:

$$\int_a^b f(x)dx = \frac{b-a}{2}\int_{-1}^{+1} f(\frac{b-a}{2}x_i + \frac{b-a}{2})dx \cong \frac{b-a}{2}\sum_{i=1}^{n} w_i f(\frac{b-a}{2}x_i + \frac{b-a}{2}) \quad (18)$$

Where f is an arbitrary function, w_i is the weight value and x_i represents the Gauss (or collocation) point. It is required to indicate the value of the shape function for each collocation point.

In the presented approach, shape functions of $\Phi1, \Phi2,$ and $\Phi3$ are formulated as follows for each collocation point of xi:

$$\Phi1 = -0.5\, xi * (1 - xi) \quad (19)$$

$$\Phi2 = (1 + xi) * (1 - xi) \quad (20)$$

$$\Phi3 = 0.5\, xi * (1 + xi) \quad (21)$$

Where xi is the value of the ith collocation point. The value of Cartesian coordinates and the distance from each arbitrary point (r), are defined as follows:

$$x = p1(1).\Phi1 + p2(1).\Phi2 + p3(1).\Phi3 \quad (22)$$

$$y = p1(2).\Phi1 + p2(2).\Phi2 + p3(2).\Phi3 \quad (23)$$

$$r = \sqrt{(x - sp(1))^2 + (y - sp(2))^2} \quad (24)$$

Where, $p1(1)$, $p2(1)$, and $p3(1)$ are x-coordinate and $p1(2)$, $p2(2)$, and $p3(2)$ are y-coordinate of the nodal points. Also, $sp(1)$ and $sp(2)$ are the x and y coordinate of the source point, respectively. With respect to the above mentioned equations, the code of integration of $u^*\phi_i$function based on normal Gauss quadrature method (10 points) approach has been provided in MATLAB.

5. Integration of G by logarithmic Gauss quad

5. 1. Coordinates and shape functions

Here the local coordinate of η is used. The value of η at the first node of the element is zero and in the last node is +1. Fig. 3 illustrates this coordinate and node’s values. As in this case, the source point is placed over the first node of 1, the singularity occurs normally. If singularity occurs in the last node (2), the value of η shall be so scaled that the last node becomes 0 and the first node goes to +1 and in the case where singularity occurs in the middle node of the element (3), it is integrated by two integrals, one of them going from mid-point to end and the other one going from mid-point to the first point.

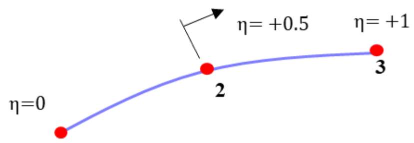

Fig. 3: Local coordinate of $\boldsymbol{\eta}$

5. 2. Shape functions

In this case, two types of shape functions are used. The first one is the normal shape function indicated previously, and the other is the singular shape function, which is indicated by Φ and Ψ respectively. Formulation of Φ is presented for the normal Gauss integration and Ψ is presented as follows:

$$\Psi1 = (\eta - 1).(2\eta - 1) \quad (25)$$

$$\Psi2 = 4\eta.(1 - \eta) \quad (26)$$

$$\Psi3 = \eta.(2\eta - 1) \quad (27)$$

5. 3. Local coordinates

For this singular treating approach, u^* is separated into three parts (singular and non-singular parts). Each of these parts shall be integrated separately. The non-singular parts can be integrated using a simple gauss quad (10 point quad) and the singular part shall be integrated by the specific weights and collocation points of the logarithmic singular quad. There are two possible options for the definition of the coordinates and calculation of the distance between an arbitrary point and the source point. The first scheme used Φi functions based on nodal points coordinates and the second one used Ψi functions (Table 1).

Table 1: Definition of the coordinates and the distance between arbitrary points

The first scheme	$x = p1(1).\Phi1 + p2(1).\Phi2 + p3(1).\Phi3$ $y = p1(2).\Phi1 + p2(2).\Phi2 + p3(2).\Phi3$ $r = \sqrt{(x - sp(1))^2 + (x - sp(2))^2}$
The second scheme	$x = p1(1).\Psi1 + p2(1).\Psi2 + p3(1).\Psi3$ $y = p1(2).\Psi1 + p2(2).\Psi2 + p3(2).\Psi3$ $r = \sqrt{(x - sp(1))\hat{}2 + (x - sp(2))\hat{}2)}$

5. 4. Jacobian of transformation

As two coordinates for integrating are used in this approach, two different transformations are required. For the first one, the coordinate is transformed to the t $(-1,+1)$ coordinate, and at the second one, the coordinate is transformed to the η axis $(0,+1)$, thus two Jacobians for transforming are required. Jacobian for normal and logarithmic integrations are defined as follows

$$J1 = \sqrt{4(A^2 + C^2).\eta(i)^2 + 4(AB + CD).\eta(i) + B^2 + D^2} \quad (28)$$

$$J2 = 0.50\, J1 \quad (29)$$

Where A, B, C and D are as follows:

$$A = 2p1(1) - 4p2(1) + 2p3(1) \quad (30)$$

$$B = -3p1(1) + 4p2(1) - p3(1) \quad (31)$$

$$C = 2p1(2) - 4p2(2) + 2p3(2) \quad (32)$$

$$D = -3p1(2) + 4p2(2) - p3(2) \quad (33)$$

6. Analytical integration

While in numerical integrations it is required to integrate singular and non-singular parts separately, using the analytical formulation can integrate the logarithmic singular function of $u^*\phi_{\mathrm{i}}$ with high accuracy. MATLAB code is also used for the analytical integration, based on the Laplacian formulation field, for calculating the singularity of $u^*\phi_{\mathrm{i}}$.

7. Hybrid Analytical-Numerical Integration Method (HINTM)

In the proposed scheme, the singular function is separated into two parts, singular and non-singular. In this regard, the proposed scheme by Smith [24] for quadratic elements has been used. Then the singular part is integrated using the analytical methods, while the non-singular part is integrated by the normal Gauss quadrature which is illustrated in section 4 of the current paper. Analytical integration of the function is performed through a developed MATLAB function which is currently used for analytical solution of the heat transfer problems and is illustrated in Section 6. The accuracy of the results is indicated in Section 8 by a numerical example.

8. Numerical example

In order to compare the capability of different schemes for the integration of $u^*\phi_i$ function, four mentioned approaches are used in examples. All of these approaches have been coded in MATLAB software to evaluate the value of G integrated separately. In the case of the first numerical example, it is considered that the singularity is induced in the first node of the element which can be generalized into other nodes too.
The obtained results of the above mentioned codes are compared. This comparison indicates that the numerical method of normal Gauss quad with 10 points is not capable of integrating the singular function of $u^*.\phi_1$ in the case of coinciding of source point on the first node. But the proposed scheme is capable of executing singular integration more efficiently in comparison with the other analytical methods.
The source point in this numerical example is located at $(0,0)$ which lies on the first node of the element. It is noteworthy that this element and source point can be arbitrary, and the only restriction is the location of the singular source point on the first node of the element.
Three elements have been used for this numerical example. In order to indicate the geometry of the numerical example, a list of the nodes is presented in Table 2, and the length of the element is compared in Fig. 4.

Table 2: Geometrical coordinates of the elements

Element	Point 1	Point 2	Point 3
E1	$p1 = (0,0)$	$p2 = (1,1)$	$p3 = (2,2)$
E2	$p1 = (0,0)$	$p2 = (2,2)$	$p3 = (4,4)$
E3	$p1 = (0,0)$	$p2 = (6,6)$	$p3 = (12,12)$

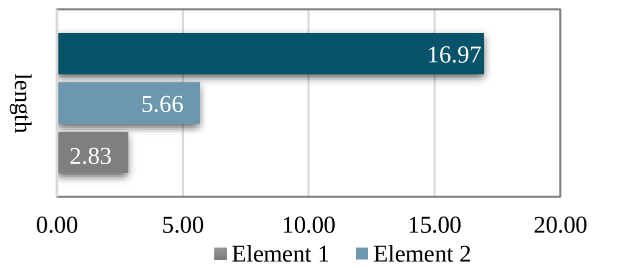

Fig. 4: Comparison of the elements length

$sp = (0,0)$ (34)

Where $sp, p1, p2, and\ p3$ are the source, first, second, and third nodal boundary points of the element respectively, and the first and the second number in the round brackets indicate the value of x and y coordinates of a point. The obtained results from the numerical and analytical schemes are presented in section 8.1, for comparison. Normal Gauss quad up to five digits shows inaccuracy by 10 points but the analytical, hybrid and logarithmic gauss methods indicated an acceptable accuracy in this numerical example.

8.1. Comparison of the results

As the selection of a method for the production of a code can be done based on the required accuracy and the computational effort below, the results of the different integration methods are compared in a list with the results of the proposed scheme (Tables 3-5). These tables indicate the results of the integration, the accuracy of the methods, and the computational efforts, respectively. Finally, based on the presented results, a conclusion has been derived for the proper method of integration to be used in BEM formulations for different purposes.

Fig. 5. demonstrates a comparison of the results for different integration methods. These methods are the Analytical Integration Method (INTM), the proposed Hybrid Analytical-Numerical Integration Method (HINTM), Normal Gauss Quadrature Method (NGM), and the specially developed Gauss Quadrature Integration Method (LGM) for logarithmically singular functions, respectively.

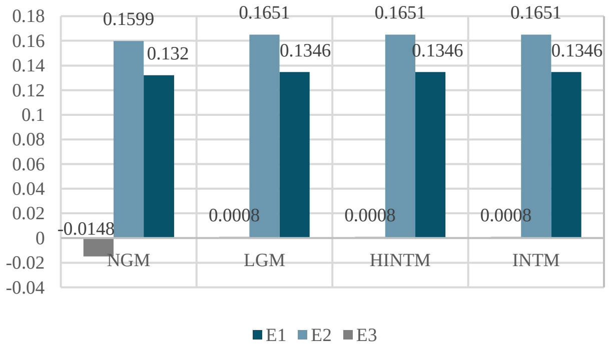

INTM: Exact value of G analytically integrated

HINTM: Value of G integrated by a hybrid analytical and numerical method

NGM: Estimated value of G integrated by normal Gauss quad method

LGM: Estimated value of G integrated by logarithmic Gauss quad method

Fig. 5: Comparison of the results for different Integration methods

As described in Table 3, up to the accuracy of float numbers, the results of HINTM (the proposed scheme) are as accurate as INTM and can be used as an alternative method with lower computational effort and the accuracy of the LGM is acceptable for the purpose of engineering problems.

Table 3: Comparison of results accuracy for different integration methods

Element	Error in each integration method			
	INTM[1]	HINTM[2]	NGM[3]	LGM[4]
E1	0	0	1.90	0
E2	0	0	3.20	0
E3	0	0	1.88E+03	0

1. Error of the analytical method – (INTM)
2. Error off the proposed hybrid method - (HINTM)
3. Error of the normal Gauss quad method – (NGM)
4. Error of the logarithmic Gauss quad method – (LGM)

The computational effort of the integrating methods is compared in Table 4. The lowest computational effort is for the NGM and LGM methods, but the NGM method due to its high error cannot be used for integration of singular cases while LGM with an elapse time of 7.1E-06 to 7.9E-06 can be an ideal method for engineering purposes. Comparing INTM and HINTM methods, computational efforts of HINT are lower which makes it an acceptable alternative method for INTM due to its acceptable accuracy and lower computational effort.

Table 4: Comparison of computational effort for different integration methods

Element	Execution time of each integration method (sec)			
	INTM[1]	HINTM[2]	NGM[3]	LGM[4]
E1	0.165552	0.144368	7.9E-06	7.9E-06
E2	0.159551	0.133851	7.1E-06	7.1E-06
E3	0.154573	0.138051	7.5E-06	7.5E-06

1. Computation time for INTM – (INTM)
2. Computation time for HINTM - (HINTM)
3. Computation time for NGM – (NGM)
4. Computation time for LGM – (LGM)

9. Heat flow example

In order to investigate the possibilities of the proposed HINTM scheme, a potential engineering problem of heat transfer in a 2 dimensional space has been solved. The solution of the potential problem is executed by the BEM as illustrate by Brebbia and Dominguez [9] and the results are compared considering the computational effort of each integration method. Fig. 6 illustrates the space of the numerical example, a square rectangular space of 36 square meters and prescribed boundary conditions.

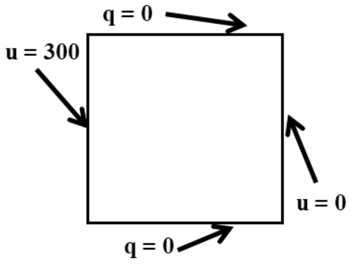

Fig. 6: Boundary conditions of numerical example 2

The body is divided into 12 boundary elements and five internal points have been assumed in the proposed body as prescribed in Table 5. Furthermore, Fig. 7 indicates the boundary elements and internal points of the body.

Table 5: Internal points positions

Point number	X location	Y location
1	2	2
2	2	4
3	3	3
4	4	2
5	4	4

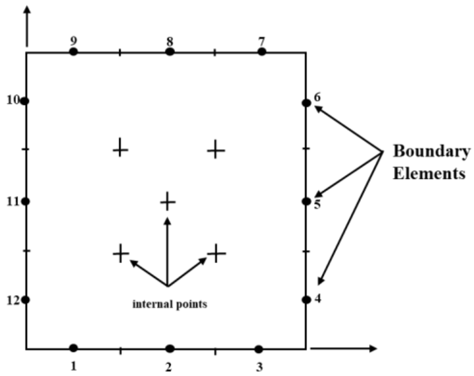

Fig. 7: Position of internal points and boundary elements

9.1. Comparison of the results

In this section, computational effort and the result of the potential problem (heat flow problem) have been compared. The computational effort of three methods, the numerical Gauss method particularly developed for logarithmic singularities, the analytical method, and the hybrid scheme (HINTM) are presented in Fig. 8. As illustrated in Fig. 8 the proposed scheme has lower computational effort compared to the normal analytical method. However, the computational time of the numerical Gauss method especially developed for logarithmic singularities is relatively lower than the proposed scheme.

Fig. 9 illustrates the analytical solution of the heat flow potential function distribution in the boundary of the numerical example [9], where u is the potential function and q is the geometrical derivative of the potential function.

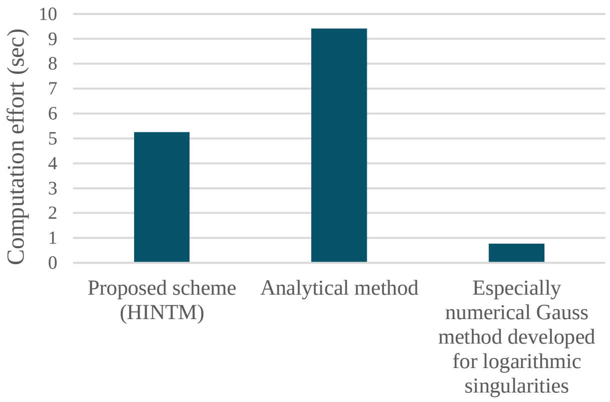

Fig. 8: Comparison of the computational efforts in different integration methods for solution of the heat flow example

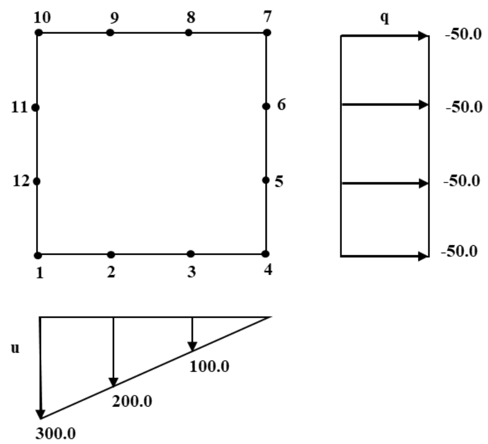

Fig. 9: Boundary solution of the potential problem

Table 6 indicates the internal solution of the heat flow problem for the steady state by various integration methods and compares the errors of each one of them.

The internal points of Table 6 are illustrated in Fig. 7, which are placed in the center and four corners of a rectangle inside the domain. The results of Table 6 reveal the acceptable accuracy of the proposed scheme in practical problems.

Table 6: Comparison of the result of the heat flow example solved through various solution methods for internal points

Point	Analytical method	HINTM	Gauss integration method	Error of hybrid scheme (HINTM) (%)	Error of Gauss integration method (%)
1	200	200.2220188	200.2220188	0.111009406	0.111009406
2	200	200.0881475	200.0881475	0.044073769	0.044073769
3	150	149.9999473	149.9999473	3.51528E-05	3.51528E-05
4	100	99.91278277	99.91278277	0.087217226	0.087217226
5	100	99.7789115	99.7789115	0.221088502	0.221088502

10. Conclusions

In this paper, the fundamental solution of Laplace's equation weighted by a shape function has been integrated for the singular case. The proposed scheme of this paper has applied the analytical and numerical methods after the separation of the singular and non-singular parts of the singular function. Furthermore, the capabilities of three integration methods, on the integration of the singular functions, have been compared with the capabilities of the proposed scheme, and the results have been investigated.

Comparing the accuracy of the results, the methods of using MATLAB analytical function and the proposed scheme, experience the most accurate results. The results of the solved numerical problems indicate that the specifically developed method for integration of logarithmically singular functions has exposed a negligible value of error which makes it an ideal method for the solution of engineering problems. However, considering the high value of error in the normal Gauss quadrature (with 10 points), its usage for real engineering problems can lead to irregular results, henceforth it has been neglected in this paper. Also, considering computational effort the Analytical Integration Method (INTM), the proposed Hybrid Analytical-Numerical Integration Method (HINTM), Normal Gauss Quadrature Method (NGM), and the specially developed Gauss Quadrature Integration Method (LGM) for logarithmically singular functions have the highest computational efforts, respectively. As a result, it is proposed to use NGM only in nonsingular cases and LGM and HINTM for the integration of logarithmically singular cases, as the case of this paper. Consequently, the proposed HINTM presents lower computational effort compared to the INTM, and its usage is proposed for high accuracies such as comparison purposes.

Further investigations can be beneficial if the usage of these integration methods is included in other engineering problems such as elastic problems.

References

[1] R. J. Astley and W. Eversman, "A finite element method for transmission in non-uniform ducts without flow: comparison with the method of weighted residuals," *Journal of Sound and Vibration,* vol. 57, pp. 367-388, 1978.

[2] B. Finlayson and L. Scriven, "The method of weighted residuals—a review," *Appl. Mech. Rev,* vol. 19, pp. 735-748, 1966.

[3] B. A. Finlayson, The method of weighted residuals and variational principles vol. 73: SIAM, 2013.

[4] A. Haji-Sheikh, E. Sparrow, and W. Minkowycz, "Heat transfer to flow through porous passages using extended weighted residuals method—a Green's function solution," *International journal of heat and mass transfer,* vol. 48, pp. 1330-1349, 2005.

[5] M. Ganz, "Finite Element Method I," 2010.

[6] T. Yang, *Finite element structural analysis* vol. 2: Prentice-Hall Englewood Cliffs, NJ, 1986.

[7] G. Beer, *Programming the boundary element method*: John Wiley & Sons, Inc., 2000.

[8] G. Beer, I. Smith, and C. Duenser, *The boundary element method with programming: for engineers and scientists*: Springer Science & Business Media, 2008.

[9] C. A. Brebbia and J. Dominguez, *Boundary elements: an introductory course*: WIT press, 1994.

[10] T. A. Cruse, *Boundary element analysis in computational fracture mechanics* vol. 1: Springer Science & Business Media, 2012.

[11] L. Gaul, M. Kögl, and M. Wagner, Boundary element methods for engineers and scientists: an introductory course with advanced topics: Springer Science & Business Media, 2013.

[12] A. Nohegoo-Shahvari, M. Kamalian, and M. Panji, "A hybrid time-domain half-plane FE/BE approach for SH-wave scattering of alluvial sites," *Engineering Analysis with Boundary Elements,* vol. 105, pp. 194-206, 2019.

[13] A. Sohrabi-Bidar, M. Kamalian, and M. K. Jafari, "Seismic response of 3-D Gaussian-shaped valleys to vertically propagating incident waves," *Geophysical Journal International,* vol. 183, pp. 1429-1442, 2010.

[14] H. Alielahi and M. Adampira, "Evaluation of 2D seismic site response due to hill-cavity interaction using boundary element technique," *Journal of Earthquake Engineering,* vol. 22, pp. 1137-1167, 2018.

[15] M. Panji, H. Koohsari, M. Adampira, H. Alielahi, and J. A. Marnani, "Stability analysis of shallow tunnels subjected to eccentric loads by a boundary element method," *Journal of Rock*

Mechanics and Geotechnical Engineering, vol. 8, pp. 480-488, 2016.

[16] A. Abdollahipour, M. F. Marji, A. Y. Bafghi, and J. Gholamnejad, "Time-dependent crack propagation in a poroelastic medium using a fully coupled hydromechanical displacement discontinuity method," *International Journal of Fracture,* vol. 199, pp. 71-87, 2016.

[17] M. Lak, M. F. Marji, A. Y. Bafghi, and A. Abdollahipour, "A coupled finite difference-boundary element method for modeling the propagation of explosion-induced radial cracks around a wellbore," *Journal of Natural Gas Science and Engineering,* vol. 64, pp. 41-51, 2019.

[18] M. F. Marji, "Numerical analysis of quasi-static crack branching in brittle solids by a modified displacement discontinuity method," *International Journal of Solids and Structures,* vol. 51, pp. 1716-1736, 2014.

[19] M. F. Marji, "Simulation of crack coalescence mechanism underneath single and double disc cutters by higher order displacement discontinuity method," *Journal of Central South University,* vol. 22, pp. 1045-1054, 2015.

[20] M. Panji, M. Kamalian, J. Asgari Marnani, and M. Jafari, "Analysing seismic convex topographies by a half-plane time-domain BEM," *Geophysical Journal International,* vol. 197, pp. 591-607, 2014.

[21] M. Panji, M. Kamalian, M. J. ASGARI, and M. Jafari, "Antiplane seismic response from semi-sine shaped valley above embedded truncated circular cavity: a time-domain half-plane BEM," 2014.

[22] M. Panji, M. Kamalian, J. A. Marnani, and M. Jafari, "Transient analysis of wave propagation problems by half-plane BEM," *Geophysical Journal International,* vol. 194, pp. 1849-1865, 2013.

[23] J. A. Crow, "Quadrature of integrands with a logarithmic singularity," *mathematics of computation,* vol. 60, pp. 297-301, 1993.

[24] R. Smith, "Simplifying integration for logarithmic singularities," *WIT Transactions on Modelling and Simulation,* vol. 14, 1970.

[25] V. Sladek, J. Sladek, and M. Tanaka, "Numerical integration of logarithmic and nearly logarithmic singularity in BEMs," *Applied Mathematical Modelling,* vol. 25, pp. 901-922, 2001.

[26] M. F. Marji, H. Hosseini-Nasab, and A. H. Kohsary, "A new cubic element formulation of the displacement discontinuity method using three special crack tip elements for crack analysis," *JP J. Solids Struct,* vol. 1, pp. 61-91, 2007.

[27] H. Haeri, K. Shahriar, M. FatehiMarji, and P. Moarefvand, "On the crack propagation analysis of rock like Brazilian disc specimens containing cracks under compressive line loading," *Latin American journal of solids and structures,* vol. 11, pp. 1400-1416, 2014.

[28] C. W. Clenshaw and A. R. Curtis, "A method for numerical integration on an automatic computer," *Numerische Mathematik,* vol. 2, pp. 197-205, 1960.

[29] B. Birgisson, E. Siebrits, and A. P. Peirce, "Elastodynamic direct boundary element methods with enhanced numerical stability properties," *International journal for numerical methods in engineering,* vol. 46, pp. 871-888, 1999.

[30] A. Tadeu, P. Santos, and E. Kausel, "Closed-form integration of singular terms for constant, linear and quadratic boundary elements. Part 1. SH wave propagation," *Engineering Analysis with Boundary Elements,* vol. 23, pp. 671-681, 1999.

[31] M. Fratantonio and J. Rencis, "Exact boundary element integrations for two-dimensional Laplace equation," *Engineering Analysis with Boundary Elements,* vol. 24, pp. 325-342, 2000.

[32] A. P. Selvadurai, Partial differential equations in mechanics 2: the biharmonic equation, Poisson's equation: Springer Science & Business Media, 2013.

[33] S. W. C. A. BREBBIA, *Boundary Element Techniques in Engineering*. LONDON, BOSTON, Sydney, Wellington, Durban,Toronto: Camelot Press Ltd, 1980.